

CreaiLayout: Siamese Multimodal Diffusion Transformer for Creative Layout-to-Image Generation

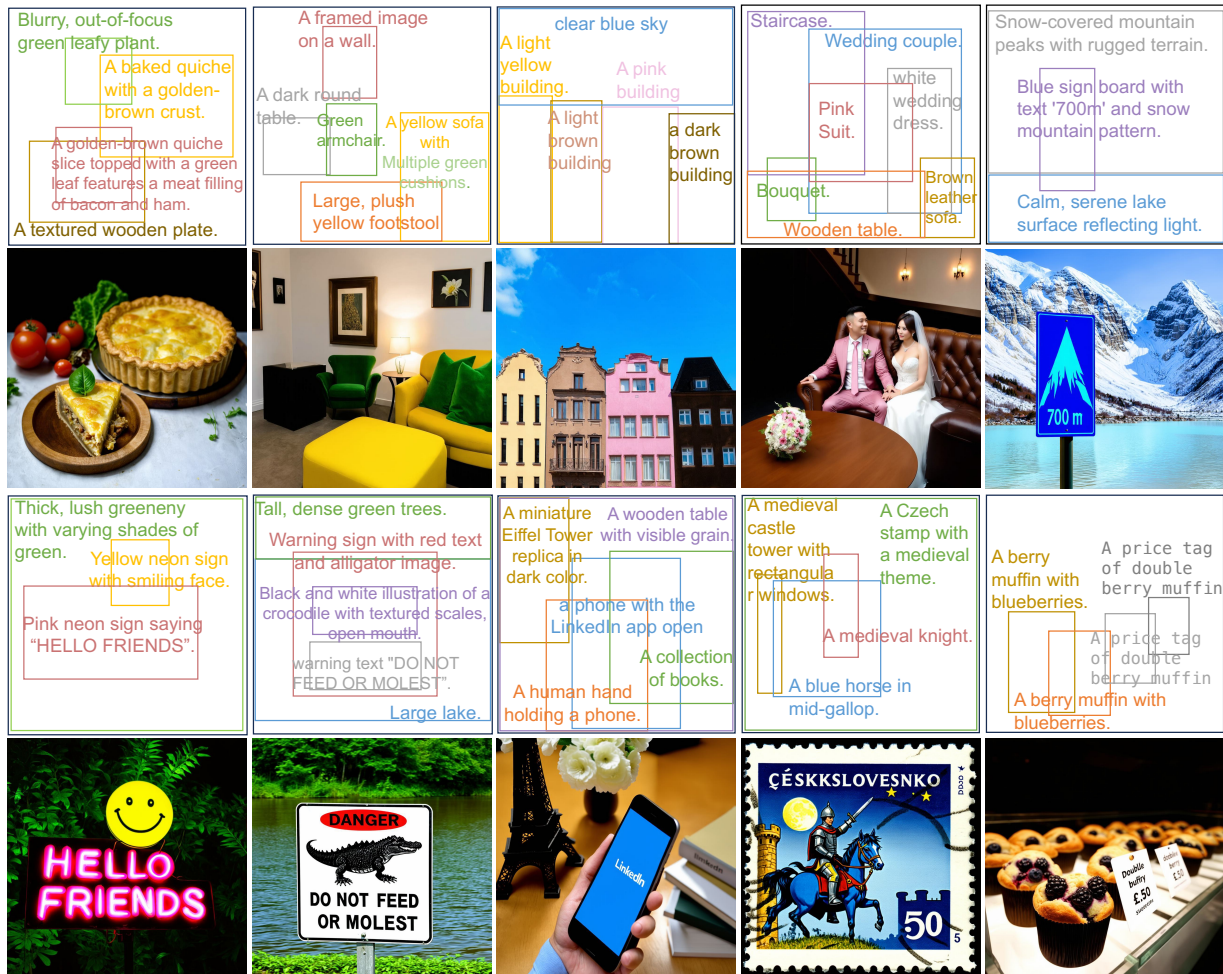
Hui Zhang^{1,2}Dexiang Hong²
Xinglong Wu²Tingwei Gao²
Zuxuan Wu^{1*}Yitong Wang²
Yu-Gang Jiang¹Jie Shao²¹Fudan University²ByteDance Inc.

Figure 1. We present a novel approach to empower MM-DiT for layout-to-image generation, achieving high-quality and fine-grained controllable generation, as evidenced by the precise rendering of complex attributes (e.g. color, texture, shape, numeracy, and text).

Abstract

Diffusion models have been recognized for their ability to generate images that are not only visually appealing but also of high artistic quality. As a result, Layout-to-Image (L2I)

generation has been proposed to leverage region-specific positions and descriptions to enable more precise and controllable generation. However, previous methods primarily focus on UNet-based models (e.g., SD1.5 and SDXL), and limited effort has explored Multimodal Diffusion Transformers (MM-DiTs), which have demonstrated powerful image generation capabilities. Enabling MM-DiT for layout-to-image gener-

* Corresponding author.

ation seems straightforward but is challenging due to the complexity of how layout is introduced, integrated, and balanced among multiple modalities. To this end, we explore various network variants to efficiently incorporate layout guidance into MM-DiT, and ultimately present SiamLayout. To inherit the advantages of MM-DiT, we use a separate set of network weights to process the layout, treating it as equally important as the image and text modalities. Meanwhile, to alleviate the competition among modalities, we decouple the image-layout interaction into a siamese branch alongside the image-text one and fuse them in the later stage. Moreover, we contribute a large-scale layout dataset, named LayoutSAM, which includes 2.7 million image-text pairs and 10.7 million entities. Each entity is annotated with a bounding box and a detailed description. We further construct the LayoutSAM-Eval benchmark as a comprehensive tool for evaluating the L2I generation quality. Finally, we introduce the Layout Designer, which taps into the potential of large language models in layout planning, transforming them into experts in layout generation and optimization. Our code, model, and dataset will be available at [Project Page](#).

1. Introduction

Text-to-image (T2I) generation [6, 38, 48, 53] has been widely applied and deeply ingrained in various fields thanks to the rapid advancement of diffusion models [20, 58]. To achieve more controllable generation, Layout-to-image (L2I) has been proposed to generate images based on layout conditions consisting of spatial location and description of entities.

Recently, multimodal diffusion transformers (MM-DiTs) [10, 32, 35, 59] have taken text-to-image generation to the next level. These models treat text as an independent modality equally important as the image and utilize MM-Attention [10] instead of cross-attention for interaction between modalities, thus enhancing prompt following. However, previous layout-to-image methods [37, 62, 72] mainly fall into UNet-based architectures [48, 53] and achieve layout control by introducing extra image-layout fusion modules between the image’s self-attention and the image-text cross-attention. While enabling MM-DiT for layout-to-image generation seems straightforward, it is challenging due to the complexity of how layout is introduced, integrated, and balanced among multiple modalities. To this end, *there is a pressing need to tailor a layout integration network for MM-DiTs*, fully unleashing their capabilities for high-quality and precisely controllable generation.

To address this issue, we explore various network variants and ultimately propose SiamLayout. Firstly, *we treat layout as an independent modality*, equally important as the image and text modalities. More specifically, we employ a separate set of transformer parameters to process the layout modality. During the forward process, the layout modality interacts with other modalities via MM-Attention and maintains self-

Layout Dataset	COCO [40]	Instance [62]	Ranni [12]	LayoutSAM
Spatial Location	✓	✓	✓	✓
Detailed Global Description	✗	✗	✓	✓
Detailed Region Description	✗	✓	✗	✓
Open-Set Entity	✗	✗	✓	✓

Table 1. Compared to previous layout datasets, LayoutSAM consists of open-set entities with fine-grained annotations.

updates. Secondly, *we decouple the interactions among the three modalities into two siamese branches: image-layout and image-text MM-Attentions*. By independently guiding the image with text and layout and then fusing them at a later stage, we alleviate competition among modalities and strengthen the guidance from the layout.

To this end, a high-quality layout dataset composed of image-text pairs and entity annotations is crucial for training the layout-to-image model. As shown in Tab. 1, the closed-set and coarse-grained nature of existing layout datasets may limit the model’s ability to generate complex attributes (e.g. color, shape, texture). Thus, we construct an automated annotation pipeline and contribute a large-scale layout dataset derived from the SAM dataset [30], named LayoutSAM. It includes 2.7M image-text pairs and 10.7M entities. Each entity includes a spatial position (*i.e.* bounding box) and a region description. The descriptions of images and entities are fine-grained, with an average length of 95.41 tokens and 15.07 tokens, respectively. We further introduce the LayoutSAM-Eval benchmark to provide a comprehensive tool for evaluating layout-to-image generation quality.

To support diverse user inputs rather than just bounding boxes of entities, we turn a large language model into a layout planner named LayoutDesigner. This model can convert and optimize various user inputs such as center points, masks, scribbles, or even a rough idea, into a harmonious and aesthetically pleasing layout.

Through comprehensive evaluations on LayoutSAM-Eval and COCO benchmarks, SiamLayout outperforms other variants and previous SOTA models by a clear margin, especially in generating entities with complex attributes, as illustrated in Fig. 1. For layout planning, LayoutDesigner shows more comprehensive and specialized capabilities compared to baseline LLMs.

2. Related Work

Text-to-Image Generation. Text-to-image generation [2, 3, 6, 13, 38, 46, 48, 53, 54] has emerged as a promising application due to its impressive capabilities. Recently, studies such as SD3 [10], SD3.5 [59], FLUX.1 [32], and Playground-v3 [41] have advanced the multimodal Diffusion Transformer architecture (MM-DiT), elevating text-to-image generation to the next level. MM-DiT significantly enhances text understanding by treating text as an independent modality, equally important as the image, and replacing traditional cross-attention with MM-Attention for modal interaction.

Layout-to-Image Generation. To achieve more precise and controllable generation, layout-to-image generation [8, 12, 14, 21, 27, 34, 37, 47, 57, 62, 65, 67, 68, 71, 72] has been proposed to generate images based on layout guidance, which includes several entities. Each entity comprises a spatial location and a region description. However, previous methods primarily focused on UNet-based architectures, and enabling MM-DiT for layout-to-image generation is challenging due to the complexity of introducing, integrating, and balancing the layout among multiple modalities. In this paper, we focus on exploring winner solutions for incorporating layout into MM-DiT, thereby fully unleashing its capabilities and achieving precisely controllable generation.

Layout Datasets. Layout datasets typically consist of image-text pairs with entity annotations. A common type [37, 68, 71] originates from COCO [40], featuring images with global descriptions and entities marked by bounding boxes and brief descriptions. Although some effort [27, 57, 62] expands descriptions using Large Language Models (LLMs) or Vision-Language Models (VLMs), they are still limited due to the close-set nature. Ranni [12] collects large-scale text-image pairs from LAION [56] and WebVision [36], moving towards an open-set layout dataset. However, entity descriptions remain coarse-grained and lack complex attributes. In this paper, we present an annotation pipeline and introduce a large-scale layout dataset containing 2.7M image-text pairs and 10.7M detailed entity annotations.

Large Language Model for Layout Generation. Layout generation [18, 22, 63] refers to the multimodal task of creating layouts for flyers, magazines, UI interfaces, or natural images. Some studies [5, 7, 11, 12, 39, 47, 49, 61, 64, 69] have explored using LLMs [1, 9, 24, 26, 60] to generate layouts based on textual descriptions, which then guide the generation of images. In this paper, we further enhance the capabilities of LLMs for generation and optimization as well as supporting user input of different granularities.

3. Methodology

3.1. Preliminaries

Latent Diffusion Models (LDMs). Latent diffusion models perform the diffusion process in the latent space, which consists of a VAE [29], text encoders, and either a UNet-based or transformer-based noise prediction model ϵ_θ . The VAE encoder \mathcal{E} encodes images \mathbf{x} into the latent space \mathbf{z} , while the VAE decoder \mathcal{D} reconstructs the latent back into images. The text encoders τ , such as CLIP [50] and T5 [51], project tokenized text prompts into text embeddings \mathbf{y} . The training objective is to minimize the following LDM loss:

$$\mathcal{L}_{LDM} = \mathbb{E}_{\mathbf{z} \sim \mathcal{E}(\mathbf{x}), \mathbf{y}, \epsilon \sim \mathcal{N}(0,1), t} \left[\|\epsilon - \epsilon_\theta(\mathbf{z}_t, t, \mathbf{y})\|_2^2 \right], \quad (1)$$

where t is time step uniformly sampled from $\{1, \dots, T\}$. The latent \mathbf{z}_t is obtained by adding noise to \mathbf{z}_0 , with the noise

ϵ sampled from the standard normal distribution $\mathcal{N}(\mathbf{0}, \mathbf{I})$.

Multimodal Diffusion Transformer. SD3/3.5 [10, 59], FLUX.1 [32], and Playground-v3 [41] instantiate noise prediction using MM-DiT, which uses two independent transformers to handle text and image embeddings separately. Unlike previous diffusion models that process different modalities through cross-attention, MM-DiT concatenates the embeddings of the image and text for the self-attention operation, referred to as MM-Attention:

$$\mathbf{z}, \mathbf{y} = \text{Self-Attention}([\mathbf{z}, \mathbf{y}]). \quad (2)$$

MM-DiT treats image and text as equally important modalities to improve prompt following [10]. In this paper, we explore incorporating layout into MM-DiTs, unleashing their potential for high-quality and precise L2I generation.

3.2. Layout-to-Image Generation

Problem Definition. Layout-to-image generation aims at precise and controllable image generation based on the instruction \mathbf{I} , which consists of a global-wise prompt condition \mathbf{p} and a region-wise layout condition \mathbf{l} , denoted as:

$$\text{Instruction: } \mathbf{I} = (\mathbf{p}, \mathbf{l}). \quad (3)$$

The layout condition includes information for N entities e , each consisting of two parts: region caption c and spatial location \mathbf{b} , denoted as:

$$\text{Layout Condition: } \mathbf{l} = [e_1, \dots, e_N], \text{ with} \quad (4)$$

$$\text{Entity: } e_n = (c_n, b_n). \quad (5)$$

In this work, we use bounding boxes to represent spatial locations, consisting of the coordinates of the top-left and bottom-right corners.

Tokenize Different Modalities. Image tokens \mathbf{h}^z are derived by patchifying the latent \mathbf{z} , and tokens \mathbf{h}^p of global caption \mathbf{p} are obtained from the text encoder τ , denoted as $\mathbf{h}^p = \tau(\mathbf{p})$. We denote the layout tokens as $\mathbf{h}^l = [h_1^l, \dots, h_N^l]$. Inspired by GLIGEN [37], each h_i^l is obtained from the layout encoder in Fig. 2:

$$h_i^l = \text{MLP}([\tau(c_i), \text{Fourier}(b_i)]) \quad (6)$$

Fourier refers to the Fourier embedding [44], $[\cdot, \cdot]$ denotes concatenation across the feature dimension, and MLP is a multi-layer perception.

Layout Integration. MM-DiT [10] allows the two modalities to interact through the following MM-Attention:

$$\mathbf{h}^{z'}, \mathbf{h}^{p'} = \text{Attention}([\mathbf{Q}^z, \mathbf{Q}^p], [\mathbf{K}^z, \mathbf{K}^p], [\mathbf{V}^z, \mathbf{V}^p]), \quad (7)$$

where $[\cdot, \cdot]$ denotes concatenation across the tokens dimension, $\mathbf{Q}^z = \mathbf{h}^z \mathbf{W}_q^z$, $\mathbf{K}^p = \mathbf{h}^p \mathbf{W}_k^p$, $\mathbf{V}^z = \mathbf{h}^z \mathbf{W}_v^z$, and \mathbf{W}_q^z , \mathbf{W}_k^p , \mathbf{W}_v^z are the weight matrices for the query, key, and value linear projection layers for image tokens, respectively. Tokens \mathbf{h}^p of the global caption \mathbf{p} are handled by the same paradigm as \mathbf{h}^z but with their own weights. $\mathbf{h}^{z'}$ and $\mathbf{h}^{p'}$ are the image and caption tokens after interaction. To this end, the next critical step is to incorporate the layout tokens \mathbf{h}^l . We explore three variants of network designs that incorporate layout tokens, as shown in Fig. 2.

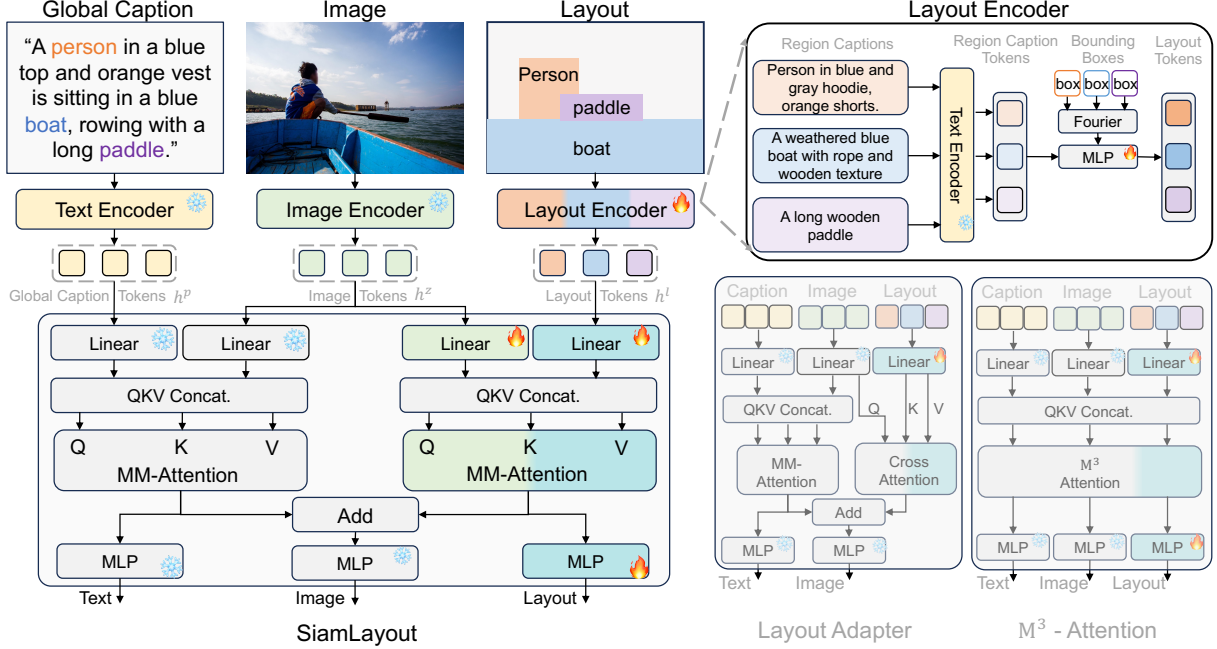


Figure 2. **An overview of the proposed pipeline.** Layout tokens are derived from the layout encoder based on spatial locations and region descriptions. SiamLayout employs separate transformer parameters to process the layout, treating it as an equally important modality as the image and text. Layout and text guide the image independently through siamese branches, and are then fused in the later stage. We experiment with two additional network variants that incorporate layout via cross-attention and M^3 -Attention. SiamLayout works best.

- *Layout Adapter.* Based on the fundamental idea of previous L2I methods [37, 62, 70, 72] introducing layout conditions in UNet-based architectures, we design extra image-layout cross-attention to incorporate layout into MM-DiT, defined as the Layout Adapter. Formally, it is represented as:

$$h_{\text{adapter}}^z = h^z + \text{Attention}(\mathbf{Q}^z, \mathbf{K}^l, \mathbf{V}^l), \quad (8)$$

where $\mathbf{K}^l = h^l \mathbf{W}_k^l$ and $\mathbf{V}^l = h^l \mathbf{W}_v^l$ are the key and values matrices from the layout tokens. \mathbf{W}_k^l and \mathbf{W}_v^l are the corresponding weight matrices. \mathbf{Q}^z is the identical query as in Eq. (7). In this way, guidance from the layout is introduced into h_{adapter}^z with fewer parameters. However, due to layout conditions not playing an equal role to the global caption condition, it may diminish the impact of layout guidance on the generation process and lead to suboptimal results.

- *M^3 -Attention.* To emphasize the importance of layout conditions, we extend the core philosophy of MM-DiT, treating layout as an independent modality equally important as the image and global caption. We employ a separate set of transformer parameters to process layout tokens and design a novel M^3 -Attention for the interaction among these three modalities:

$$h_{m^3}^z, h_{m^3}^p, h_{m^3}^l = \text{Attention}([\mathbf{Q}^z, \mathbf{Q}^p, \mathbf{Q}^l], [\mathbf{K}^z, \mathbf{K}^p, \mathbf{K}^l], [\mathbf{V}^z, \mathbf{V}^p, \mathbf{V}^l]), \quad (9)$$

where $\mathbf{Q}^l = h^l \mathbf{W}_q^l$, $\mathbf{K}^l = h^l \mathbf{W}_k^l$ and $\mathbf{V}^l = h^l \mathbf{W}_v^l$ are the query, key and values matrices from the layout tokens.

\mathbf{W}_q^l , \mathbf{W}_k^l and \mathbf{W}_v^l are the corresponding independent weight matrices. We concatenate these three modalities in the token dimension and then facilitate interaction among them through self-attention. During the generation process, the layout condition acts as an independent modality, constantly interacting with other modalities and maintaining self-updates. Although this design seems promising, we found that in the attention map of M^3 -Attention, the similarity between layout and image is much lower than that between the caption and image (as shown in Fig. 3 (a)), resulting in the layout having much less influence on the image compared to the global caption. We refer to this phenomenon as “modality competition”, which can be attributed to the fact that layout, as a new modality, has not been pre-trained and aligned on large-scale paired datasets like the global caption and image.

- *SiamLayout.* Finally, in order to retain the advantages of MM-Attention in multimodal interaction while mitigating competition among them, we propose a new layout fusion network named SiamLayout. As shown in Fig. 2, we decouple M^3 -Attention into two isomorphic MM-Attention branches, *i.e.* siamese branches, to handle image-text and image-layout interactions independently and simultaneously. The MM-Attention between image and layout can be formally denoted as:

$$h^{z''}, h^{l'} = \text{Attention}([\mathbf{Q}^{z'}, \mathbf{Q}^l], [\mathbf{K}^{z'}, \mathbf{K}^l], [\mathbf{V}^{z'}, \mathbf{V}^l]), \quad (10)$$

where $\mathbf{Q}^{z'}$, $\mathbf{K}^{z'}$ and $\mathbf{V}^{z'}$ are the new query, key, and value matrices obtained from the image token, with weight ma-

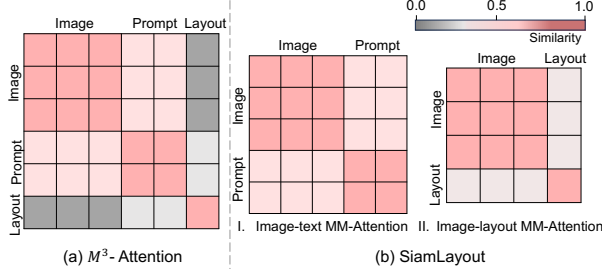


Figure 3. **Attention maps of M^3 -Attention and SiamLayout.** (a) The layout’s influence on image generation is much lower compared to the text due to lower similarity. (b) SiamLayout decouples (a) into two independent MM-Attentions for image-text and image-layout, enabling equal guidance from both layout and text.

trices different from those in Eq. (7). The final image tokens are the fusion of text-guided and layout-guided image tokens: $\mathbf{h}_{\text{siamese}}^z = \mathbf{h}^{z'} + \mathbf{h}^{z''}$. Since the guidance from the layout and global caption has been decoupled—being independent in space and parallel in time—the issue of modality competition is significantly mitigated. As shown in Fig. 3 (b), in the attention map of image-layout MM-Attention, the similarity between layout and image increases continually during training as layout takes a dominant role here.

In this paper, SiamLayout is chosen as the network that incorporates layout into MM-DiT, and our primary experiments are conducted on it.

Training and Inference. We freeze the pre-trained model and only train the newly introduced parameters θ' using the following loss function:

$$\mathcal{L}_{\text{layout}} = \mathbb{E}_{\mathbf{z}, \mathbf{p}, \mathbf{l}, t, \epsilon \sim \mathcal{N}(0,1)} \left[\left\| \epsilon - \epsilon_{\{\theta, \theta'\}}(\mathbf{z}_t, t, \mathbf{p}, \mathbf{l}) \right\|_2^2 \right]. \quad (11)$$

Here, we employ two strategies to accelerate the convergence of the model: I) Biased sampling of time steps: Since layout pertains to the structural content of images, which is primarily generated during the larger time steps, we sample time steps with a 70% probability from a normal distribution $\mathcal{N}(0.7 * T, T)$ and with a 30% probability from $\mathcal{N}(0, T)$. II) Region-aware loss: We enhance the model’s focus on areas specified by the layout by assigning greater weight to the region loss $\mathcal{L}_{\text{region}}$ associated with the regions localized by the bounding boxes in the latent space. The updated loss is:

$$\mathcal{L}'_{\text{layout}} = \mathcal{L}_{\text{layout}} + \lambda_{\text{region}} \times \mathcal{L}_{\text{region}}, \quad (12)$$

where λ_{region} modulates the importance of $\mathcal{L}_{\text{region}}$. During the inference phase, we perform layout-conditioned denoising only in the first 30% of the steps [37].

3.3. Layout Dataset and Benchmark

Layout Dataset. As there is no large-scale and fine-grained layout dataset explicitly designed for layout-to-image generation, we collect 2.7 million image-text pairs

with 10.7 million regional spatial-caption pairs derived from the SAM Dataset [30], named LayoutSAM. We design automatic schemes and strict filtering rules to annotate layout and clean noisy data, with the following five parts:

I) Image Filtering: We employ the LAION-Aesthetics predictor [33] to curate a high visual quality subset from SAM, selecting images in the top 50% of aesthetic scores.

II) Global Caption Annotation: As the SAM dataset does not provide descriptions for each image, we generate detailed descriptions using a Vision-Language Model (VLM) [16]. The average length of the captions is 95.41 tokens.

III) Entity Extraction: Existing SoTA open-set grounding models [42, 52] prefer to detect entities through a list of short phrases rather than dense captions. Thus, we utilize a Large Language Model [43] to derive brief descriptions of main entities from dense captions via in-context learning. The average length of the brief descriptions is 2.08 tokens.

IV) Entity Spatial Annotation: We use Grounding DINO [42] to annotate bounding boxes of entities and design filtering rules to clean noisy data. Following previous work [68, 71], we first filter out bounding boxes that occupy less than 2% of the total image area, then only retain images with 3 to 10 bounding boxes.

V) Region Caption Recaptioning: At this point, we have the spatial locations and brief captions for each entity. We use a VLM [45] to generate fine-grained descriptions with complex attributes for each entity based on its visual content and brief description. The average length of these detailed descriptions is 15.07 tokens.

Layout-to-Image Benchmark. The LayoutSAM-Eval benchmark serves as a comprehensive tool for evaluating L2I generation quality collected from a subset of LayoutSAM. It comprises a total of 5,000 layout data. We evaluate L2I generation quality using LayoutSAM-Eval from two aspects:

- *Region-wise quality.* This aspect is evaluated for adherence to spatial and attribute accuracy via VLM’s [45] Visual Question Answering (VQA). For each entity, spatially, the VLM evaluates whether the entity exists within the bounding box; for attributes, the VLM assesses whether the entity matches the color, text, and shape mentioned in the detailed descriptions.
- *Global-wise quality.* This aspect scores based on visual quality and global caption following, across multiple metrics including recently proposed scoring models like IR score [66] and Pick score [31], as well as traditional metrics such as CLIP [50], FID [19] and IS [55] scores. For more details on the proposed dataset and benchmark, please refer to the supplementary materials.

3.4. Layout Designer

Recent studies [5, 11, 12, 61, 64, 69] have revealed that LLMs [1, 9, 24, 60] exhibit expertise in layout planning due to their extensive training on multiple domains. Inspired by

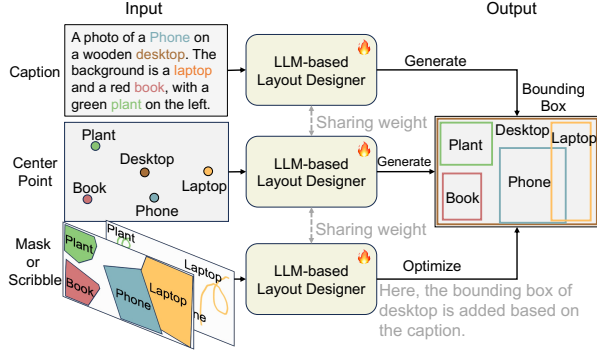


Figure 4. An overview of layout generation and optimization.

this, we further tame a LLM into a more comprehensive and professional layout designer M_l . As shown in Fig. 4, M_l is capable of executing two types of layout planning based on inputs of varying granularity:

- *Generation for coarse-grained inputs.* For user inputs with only a global caption, M_l designs from scratch based on the caption to determine which entities compose the layout and generates appropriate bounding boxes for these entities; for cases where the description and centroid coordinates (x_0, y_0) of each entity are provided, M_l designs harmonious bounding boxes based on this information.
- *Optimization for fine-grained inputs.* For entities provided with detailed spatial information, such as masks and scribbles, we first transform them into bounding boxes according to predefined rules, then employ M_l to further optimize the layout based on the global caption and the descriptions of the entities, including additions, deletions, and modifications of the bounding boxes.

To enhance the expertise of M_l , we construct 180,000 paired layout design data from LayoutSAM and fine-tune the pre-trained LLM [43] using LoRA [23] with cross-entropy loss.

4. Experiments

4.1. Experimental Details

Layout-to-Image Generation. We conduct experiments on two types of datasets: the fine-grained open-set LayoutSAM and the coarse-grained closed-set COCO 2017 [40]. For LayoutSAM, we train on 2.7 million image-text pairs with 10.7 million entities and conduct evaluations on LayoutSAM-Eval, which includes 5,000 prompts with detailed entity annotations. We measure generation quality using the metrics outlined in Sec. 3.3. For COCO, following previous work [68, 71], we filter out bounding boxes smaller than 2% of the total image area and images containing dense bounding boxes and crowds, resulting in 61,002 training images and 2,565 validation images. We use the YOLO-v11-x [28] to validate the model’s layout adherence by detecting objects in the generated images and then calculating AP, AP⁵⁰, and AR against the ground truth. We use FID, CLIP

score, and IS to measure the global image quality.

Text-to-Image Generation. We conduct experiments on the T2I-CompBench [25] and evaluate image quality from five aspects: spatial, color, shape, texture, and numeracy.

Layout Generation and Optimization. We construct 180,000 training sets based on the LayoutSAM training set for three types of user input and layout pairs: caption-layout pairs, center point-layout pairs, and suboptimal layout-layout pairs. Similarly, we construct 1,000 validation sets for each of these tasks from LayoutSAM-Eval.

Implementation Details. We employ experiments on SD3-medium, and the extra parameters introduced by SiamLayout amount to 1.28B. The training resolution for the LayoutSAM dataset is 1024×1024 , and 512×512 for COCO. We utilize the AdamW optimizer with a fixed learning rate of $5e-5$ and train the model for 600,000 iterations with a batch size of 16. We train SiamLayout with 8 A800-40G GPUs for 7 days. The value of λ_{region} is set to 2. LayoutDesigner is fine-tuned on Llama-3.1-8B-Instruct [9] for one day using one A800-40G GPU.

4.2. Evaluation on Layout-to-Image Generation

Fine-Grained Open-set L2I. Tab. 2 presents the quantitative results of SiamLayout on the fine-grained open-set LayoutSAM-Eval, including metrics of region-wise quality and global-wise quality. SiamLayout not only surpasses the current SOTA in terms of spatial response but also exhibits more precise responses in attributes such as color, texture, and shape. By fully unleashing the power of MM-DiT, SiamLayout also demonstrates a dominant advantage in overall image quality. This is further confirmed by the qualitative results in Fig. 5, showing that SiamLayout achieves more accurate and aesthetically appealing attribute rendering in the regions localized by the bounding boxes, including the rendering of shapes, colors, textures, text, and portraits.

Coarse-Grained Closed-set L2I. We train and evaluate SiamLayout on COCO to confirm its generalization in coarse-grained closed-set layout-to-image generation, as shown in Tab. 3. In terms of image quality, SiamLayout outperforms previous methods by a clear margin on CLIP, FID, and IS metrics, thanks to the tailored framework that unleashes the capabilities of MM-DiT. In terms of spatial positioning response, SiamLayout is slightly inferior to InstanceDiff. We attribute this to two factors: I) The training dataset of InstanceDiff is a more fine-grained COCO dataset, with per-entity fine-grained attribute annotations; II) InstanceDiff generates each entity separately and then combines them, achieving more precise control at the cost of increased time and computational resources.

LayoutSAM-Eval	Region-wise Quality				Global-wise Quality				
	Spatial \uparrow	Color \uparrow	Texture \uparrow	Shape \uparrow	IR \uparrow [66]	Pick \uparrow [31]	CLIP \uparrow	FID \downarrow	IS \uparrow
Real Images	98.95	98.45	98.90	98.80	-	-	-	-	-
GLIGEN [37]	77.53	49.41	55.29	52.72	-10.31	20.78	<u>32.42</u>	21.92	<u>20.57</u>
Ranni [12]	41.38	24.10	25.57	23.35	-28.46	20.49	31.40	27.24	19.81
MIGC [72]	85.66	66.97	71.24	69.06	-13.72	20.71	31.36	21.19	19.65
InstanceDiff [62]	<u>87.99</u>	<u>69.16</u>	<u>72.78</u>	<u>71.08</u>	<u>9.14</u>	<u>21.01</u>	31.40	<u>19.67</u>	20.02
Be Yourself [8]	53.99	31.73	35.26	32.75	-12.31	20.20	31.02	28.10	17.98
SiamLayout	92.67	74.45	77.21	75.93	69.47	22.02	34.01	19.10	22.04
<i>vs. prev. SoTA</i>	+4.68	+5.29	+4.43	+4.85	+60.33	+1.01	+1.59	+0.57	+1.47

Table 2. Quantitative comparison on the LayoutSAM-Eval. **Bold** and underline represent the best and second best methods, respectively.

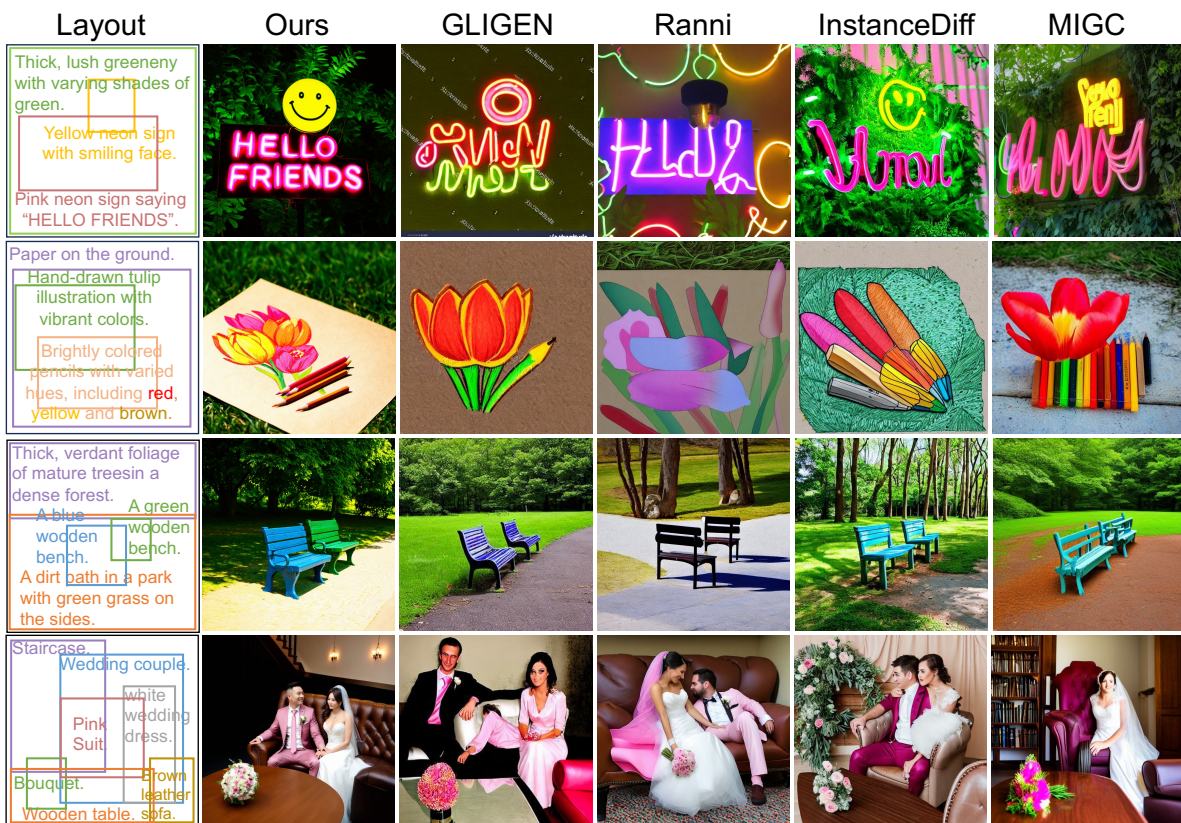


Figure 5. Qualitative results on LayoutSAM-Eval. SiamLayout outperforms previous methods by a clear margin in generating entities with complex attributes like color, texture, text, and portraits.

4.3. Evaluation on Text-to-Image Generation

To further validate the impact of incorporating layout on text-to-image generation, we conduct experiments on the T2I-CompBench [25]. For the prompts, we first use LLM to plan the layout, which is then used to generate images via SiamLayout. Tab. 4 reveals that, by introducing layout to provide further guidance signals for image generation,

SD3 has seen a significant improvement in spatial adherence (from 32.00 to 47.36). Additionally, the benefits of layout are also reflected in the improved adherence to prompts regarding color, shape, texture, and the number of objects.

4.4. Evaluation on Layout Planning

To validate the capability of layout generation and optimization, we compare LayoutDesigner fine-tuned on Llama3.1

COCO 2017	Spatial			Global-wise Quality		
	AP \uparrow	AP ⁵⁰ \uparrow	AR \uparrow	CLIP \uparrow	FID \downarrow	IS \uparrow
GLIGEN [37]	42.1	66.8	37.2	<u>30.25</u>	30.68	26.76
MIGC [72]	39.1	66.0	36.8	28.60	31.43	26.14
InstanceDiff [62]	51.9	71.9	43.7	30.04	<u>29.94</u>	<u>27.23</u>
Ranni [12]	14.7	22.3	17.0	30.02	31.94	24.44
SiamLayout	<u>47.8</u>	<u>69.8</u>	<u>42.1</u>	33.32	29.27	30.26

Table 3. Evaluation on coarse-grained COCO benchmark

T2I-CompBench	Spatial \uparrow	Color \uparrow	Shape \uparrow	Texture \uparrow	Numeracy \uparrow
Attn-Exct [4]	14.55	64.00	45.17	59.63	47.67
SDXL [48]	21.33	58.79	46.87	52.99	49.88
pixart- α [6]	20.64	66.90	49.27	64.77	50.58
DALLE-3 [3]	28.65	77.85	62.05	70.36	<u>58.80</u>
SD3 [10]	<u>32.00</u>	<u>81.32</u>	58.85	<u>73.34</u>	58.34
Ours	47.36	83.24	<u>61.32</u>	75.51	62.15

Table 4. Quantitative results on T2I-CompBench.

Layout Planning	On global caption		On center point		On bounding box	
	Acc \uparrow	Quality \uparrow	Acc \uparrow	Quality \uparrow	Acc \uparrow	Quality \uparrow
Gemma-7b-it [15]	64.79	46.33	96.14	53.46	98.83	65.10
Qwen2.5-7b-it [17]	45.09	53.49	75.36	50.63	96.50	63.22
MiniCPM3-4b [45]	70.71	55.80	66.72	<u>59.24</u>	83.25	61.57
Llama3.1-8b-it [43]	50.11	55.09	73.35	50.22	97.68	<u>65.40</u>
GPT4-Turbo [1]	<u>76.60</u>	<u>60.03</u>	<u>99.53</u>	57.41	<u>99.96</u>	65.34
LayoutDesigner	100.0	66.46	100.0	65.29	100.0	68.52
vs. prev. SOTA	+23.40	+6.43	+0.47	+6.05	+0.04	+3.12
vs. w/o. SFT	+49.89	+11.37	+26.65	+15.07	+2.32	+3.12

Table 5. Quantitative comparison of different layout planners.

with the latest LLMs, as presented in Tab. 5. Accuracy measures the correctness of the generated bounding boxes, including ensuring that the coordinates of the top-left corner are less than those of the bottom-right corner and that the bounding box does not exceed the image boundaries. Quality refers to the IR score of the image generated according to the planned layout, which is used to reflect the rationality and harmony of the layout. In terms of format accuracy, LayoutDesigner shows significant improvement over the vanilla Llama and clearly outperforms the previous SOTA. Additionally, as the LayoutDesigner contributes more aesthetically pleasing layouts, the generated images possess higher quality. Fig. 7 further confirms this, showing that layouts generated by Llama often fail to meet formatting standards or miss key elements, while those generated by GPT4-Turbo often violate fundamental physical laws (e.g. overly small objects). In contrast, images generated from layouts designed by LayoutDesigner exhibit better quality as the layouts are more harmonious and aesthetically pleasing.

4.5. Ablation Study

Ablations on Network Design. We explore three network variants aimed at integrating layout guidance into MM-DiT. Tab. 6 illustrates the accuracy of layout adherence of these designs. Compared to the vanilla SD3, Layout Adapter enhances the model’s adherence to spatial locations and attributes by introducing cross-attention between the image and layout. However, as shown in Fig. 6, it falls short when dealing with complex and fine-grained color, quantity, and texture requirements. We attribute this to the fact that the layout is not considered an independent modality equally important as the global caption and image, which limits the potential of layout guidance. The initial intention behind designing M³-Attention is to make layout, image, and caption play an equal role. However, due to the competition among these modalities in the attention map of M³-Attention, layout modality consistently is at a disadvantage, which is reflected in both quantitative and qualitative results as lower layout responsiveness. SiamLayout decouples M³-Attention into two independent and parallel MM-Attention branches: image-text and image-layout. This design allows each branch to play a significant role without interfering with each other, jointly contributing to precise responses to spatial locations and complex attributes.

	Spatial \uparrow	Color \uparrow	Texture \uparrow	Shape \uparrow
Stable Diffusion 3	78.70	59.22	60.66	58.73
w/ Layout Adapter	<u>88.43</u>	<u>71.67</u>	<u>73.56</u>	<u>72.61</u>
w/ M3-Attention	79.15	60.19	62.96	61.29
w/ SiamLayout	92.67	74.45	77.21	75.93

Table 6. Ablation study on different network variants.

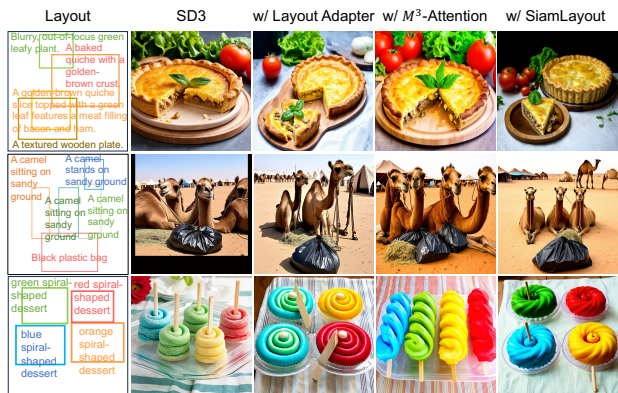


Figure 6. Qualitative results of three network variants.

The Impact of Training Strategies. In Fig. 8, we explore the impact of two strategies introduced during training on SiamLayout: biased time step sampling and region-aware loss. With the region-aware loss \mathcal{L}_{region} , the model focuses

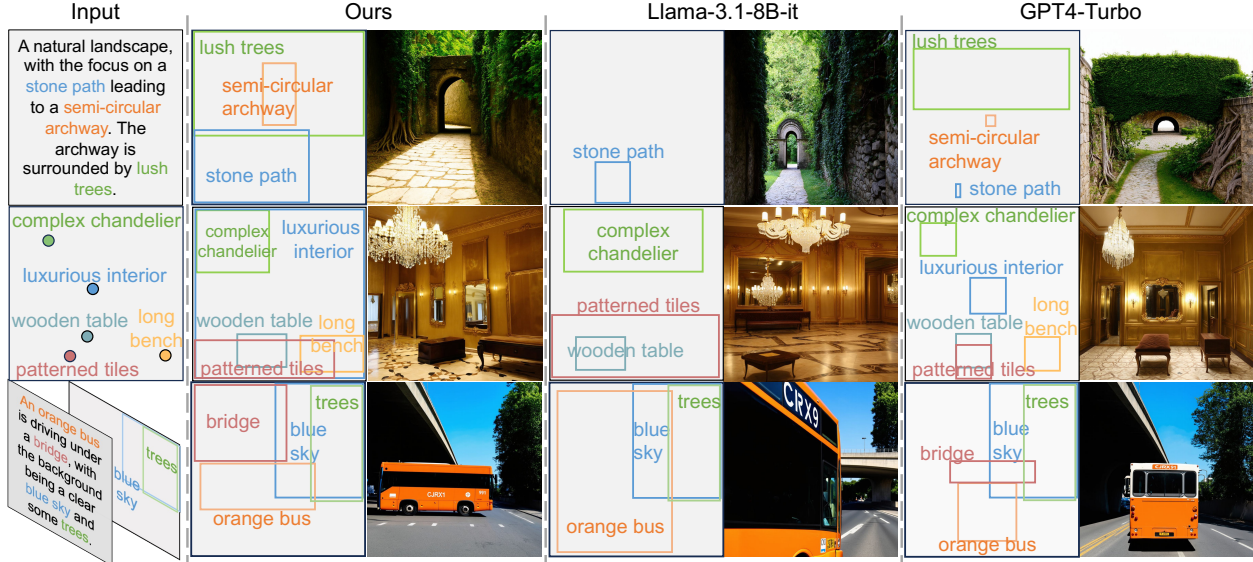


Figure 7. Qualitative comparison of different layout planners.

more on the areas localized by the layout, accelerating the model’s convergence. In addition, layout predominantly guides structural content, which is mainly generated at larger time steps. Thus, sampling larger time steps with a higher probability (*i.e.* biased time step sampling) also effectively speeds up the model’s convergence.

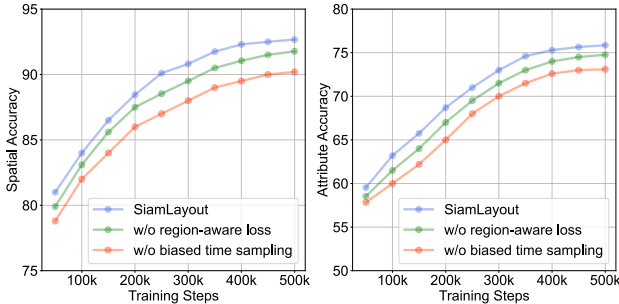


Figure 8. Ablation study on different training strategies.

5. Conclusion

We presented SiamLayout, which treats layout as an independent modality and guides image generation through an image-layout branch that is siamese to the image-text branch. SiamLayout unleashes the power of MM-DiT to achieve high-quality, accurate layout-to-image generation, and significantly outperforms previous work in generating complex attributes such as color, shape, and text. Additionally, we introduced LayoutSAM, a large-scale layout dataset with 2.7M image-text pairs and 10.7M entities, along with LayoutSAM-Eval to assess generation quality. Finally, we proposed LayoutDesigner, which tames a large language model into a professional layout planner capable of handling user inputs of varying granularity.

Limitation and Future Work. We introduce a large language model for layout planning, which brings extra computation costs. Integrating layout planning with layout-to-image generation into an end-to-end model is an important direction for future research. Additionally, the automatic annotation pipeline introduces noisy data mainly caused by the object detection model, so its impact on the performance of the layout-to-image model needs to be further studied.

References

- [1] Josh Achiam, Steven Adler, Sandhini Agarwal, Lama Ahmad, Ilge Akkaya, Florencia Leoni Aleman, Diogo Almeida, Janko Altenschmidt, Sam Altman, Shyamal Anadkat, et al. Gpt-4 technical report. *arXiv preprint arXiv:2303.08774*, 2023. 3, 5, 8
- [2] Fan Bao, Shen Nie, Kaiwen Xue, Yue Cao, Chongxuan Li, Hang Su, and Jun Zhu. All are worth words: A vit backbone for diffusion models. In *CVPR*, 2023. 2
- [3] James Betker, Gabriel Goh, Li Jing, Tim Brooks, Jianfeng Wang, Linjie Li, Long Ouyang, Juntang Zhuang, Joyce Lee, Yufei Guo, et al. Improving image generation with better captions. *Computer Science*. <https://cdn.openai.com/papers/dall-e-3.pdf>, 2023. 2, 8
- [4] Hila Chefer, Yuval Alaluf, Yael Vinker, Lior Wolf, and Daniel Cohen-Or. Attend-and-excite: Attention-based semantic guidance for text-to-image diffusion models. *ACM Transactions on Graphics (TOG)*, 2023. 8
- [5] Jingye Chen, Yupan Huang, Tengchao Lv, Lei Cui, Qifeng Chen, and Furu Wei. Textdiffuser-2: Unleashing the power of language models for text rendering. In *ECCV*, 2024. 3, 5
- [6] Junsong Chen, YU Jincheng, GE Chongjian, Lewei Yao, Enze Xie, Zhongdao Wang, James Kwok, Ping Luo, Huchuan Lu, and Zhenguo Li. Pixart- α : Fast training of diffusion

- transformer for photorealistic text-to-image synthesis. In *ICLR*, 2024. 2, 8
- [7] Jaemin Cho, Abhay Zala, and Mohit Bansal. Visual programming for step-by-step text-to-image generation and evaluation. In *NeurIPS*, 2023. 3
- [8] Omer Dahary, Or Patashnik, Kfir Aberman, and Daniel Cohen-Or. Be yourself: Bounded attention for multi-subject text-to-image generation. In *ECCV*, 2024. 3, 7
- [9] Abhimanyu Dubey, Abhinav Jauhri, Abhinav Pandey, Abhishek Kadian, Ahmad Al-Dahle, Aiesha Letman, Akhil Mathur, Alan Schelten, Amy Yang, Angela Fan, et al. The llama 3 herd of models. *arXiv preprint arXiv:2407.21783*, 2024. 3, 5, 6
- [10] Patrick Esser, Sumith Kulal, Andreas Blattmann, Rahim Entezari, Jonas Müller, Harry Saini, Yam Levi, Dominik Lorenz, Axel Sauer, Frederic Boesel, et al. Scaling rectified flow transformers for high-resolution image synthesis. *arXiv preprint arXiv:2403.03206*, 2024. 2, 3, 8
- [11] Weixi Feng, Wanrong Zhu, Tsu-jui Fu, Varun Jampani, Arjun Akula, Xuehai He, Sugato Basu, Xin Eric Wang, and William Yang Wang. Layoutgpt: Compositional visual planning and generation with large language models. In *NeurIPS*, 2023. 3, 5
- [12] Yutong Feng, Biao Gong, Di Chen, Yujun Shen, Yu Liu, and Jingren Zhou. Ranni: Taming text-to-image diffusion for accurate instruction following. In *CVPR*, 2024. 2, 3, 5, 7, 8
- [13] Peng Gao, Le Zhuo, Ziyi Lin, Chris Liu, Junsong Chen, Ruoyi Du, Enze Xie, Xu Luo, Longtian Qiu, Yuhang Zhang, et al. Lumina-t2x: Transforming text into any modality, resolution, and duration via flow-based large diffusion transformers. *arXiv preprint arXiv:2405.05945*, 2024. 2
- [14] Biao Gong, Siteng Huang, Yutong Feng, Shiwei Zhang, Yuyuan Li, and Yu Liu. Check locate rectify: A training-free layout calibration system for text-to-image generation. In *CVPR*, 2024. 3
- [15] Google. Gemma-7b-it. <https://huggingface.co/google/gemma-7b-it>, 2024. 8
- [16] Alibaba Group. Qwen-vl-chat-finetuned-dense-captioner. <https://modelscope.cn/models/Tongyi-DataEngine/Qwen-VL-Chat-Finetuned-Dense-Captioner>, 2024. 5, 1
- [17] Alibaba Group. Qwen2.5-7b-it. <https://huggingface.co/Qwen/Qwen2.5-7B-Instruct>, 2024. 8
- [18] Julian Jorge Andrade Guerreiro, Naoto Inoue, Kento Masui, Mayu Otani, and Hideki Nakayama. Layoutflow: Flow matching for layout generation. In *ECCV*, 2024. 3
- [19] Martin Heusel, Hubert Ramsauer, Thomas Unterthiner, Bernhard Nessler, and Sepp Hochreiter. Gans trained by a two time-scale update rule converge to a local nash equilibrium. In *NeurIPS*, 2017. 5
- [20] Jonathan Ho, Ajay Jain, and Pieter Abbeel. Denoising diffusion probabilistic models. In *NeurIPS*, 2020. 2
- [21] Jiun Tian Hoe, Xudong Jiang, Chee Seng Chan, Yap-Peng Tan, and Weipeng Hu. Interactdiffusion: Interaction control in text-to-image diffusion models. In *CVPR*, 2024. 3
- [22] Daichi Horita, Naoto Inoue, Kotaro Kikuchi, Kota Yamaguchi, and Kiyoharu Aizawa. Retrieval-augmented layout transformer for content-aware layout generation. In *CVPR*, 2024. 3
- [23] Edward J Hu, Yelong Shen, Phillip Wallis, Zeyuan Allen-Zhu, Yuanzhi Li, Shean Wang, Lu Wang, and Weizhu Chen. Lora: Low-rank adaptation of large language models. *arXiv preprint arXiv:2106.09685*, 2021. 6
- [24] Shengding Hu, Yuge Tu, Xu Han, Chaoqun He, Ganqu Cui, Xiang Long, Zhi Zheng, Yewei Fang, Yuxiang Huang, Weilin Zhao, et al. Minicpm: Unveiling the potential of small language models with scalable training strategies. *arXiv preprint arXiv:2404.06395*, 2024. 3, 5
- [25] Kaiyi Huang, Kaiyue Sun, Enze Xie, Zhenguo Li, and Xihui Liu. T2i-compbench: A comprehensive benchmark for open-world compositional text-to-image generation. In *NeurIPS*, 2023. 6, 7
- [26] Binyuan Hui, Jian Yang, Zeyu Cui, Jiayi Yang, Dayiheng Liu, Lei Zhang, Tianyu Liu, Jiajun Zhang, Bowen Yu, Kai Dang, et al. Qwen2. 5-coder technical report. *arXiv preprint arXiv:2409.12186*, 2024. 3
- [27] Chengyou Jia, Minnan Luo, Zhuohang Dang, Guang Dai, Xiaojun Chang, Mengmeng Wang, and Jingdong Wang. Ssmg: Spatial-semantic map guided diffusion model for free-form layout-to-image generation. In *AAAI*, 2024. 3
- [28] Rahima Khanam and Muhammad Hussain. Yolov11: An overview of the key architectural enhancements. *arXiv preprint arXiv:2410.17725*, 2024. 6
- [29] Diederik P Kingma. Auto-encoding variational bayes. *arXiv preprint arXiv:1312.6114*, 2013. 3
- [30] Alexander Kirillov, Eric Mintun, Nikhila Ravi, Hanzi Mao, Chloe Rolland, Laura Gustafson, Tete Xiao, Spencer Whitehead, Alexander C Berg, Wan-Yen Lo, et al. Segment anything. In *ICCV*, 2023. 2, 5, 1
- [31] Yuval Kirstain, Adam Polyak, Uriel Singer, Shahbuland Matiana, Joe Penna, and Omer Levy. Pick-a-pic: An open dataset of user preferences for text-to-image generation. *arXiv preprint arXiv:2305.01569*, 2023. 5, 7
- [32] Black Forest Labs. Flux. <https://blackforestlabs.ai/announcing-black-forest-labs>, 2024. 2, 3
- [33] LAION. Laion-aesthetics v2. <https://github.com/christophschuhmann/improved-aesthetic-predictor>, 2022. 5, 1
- [34] Phillip Y Lee, Taehoon Yoon, and Minhyuk Sung. Groundit: Grounding diffusion transformers via noisy patch transplantation. *arXiv preprint arXiv:2410.20474*, 2024. 3
- [35] Daiqing Li, Aleks Kamko, Ehsan Akhgari, Ali Sabet, Linmiao Xu, and Suhail Doshi. Playground v2. 5: Three insights towards enhancing aesthetic quality in text-to-image generation. *arXiv preprint arXiv:2402.17245*, 2024. 2
- [36] Wen Li, Limin Wang, Wei Li, Eirikur Agustsson, and Luc Van Gool. Webvision database: Visual learning and understanding from web data. *arXiv preprint arXiv:1708.02862*, 2017. 3
- [37] Yuheng Li, Haotian Liu, Qingyang Wu, Fangzhou Mu, Jianwei Yang, Jianfeng Gao, Chunyuan Li, and Yong Jae Lee. Gligen: Open-set grounded text-to-image generation. In *CVPR*, 2023. 2, 3, 4, 5, 7, 8

- [38] Zhimin Li, Jianwei Zhang, Qin Lin, Jiangfeng Xiong, Yanxin Long, Xincheng Deng, Yingfang Zhang, Xingchao Liu, Minbin Huang, Zedong Xiao, et al. Hunyuan-dit: A powerful multi-resolution diffusion transformer with fine-grained chinese understanding. *arXiv e-prints*, 2024. 2
- [39] Long Lian, Boyi Li, Adam Yala, and Trevor Darrell. Llm-grounded diffusion: Enhancing prompt understanding of text-to-image diffusion models with large language models. *TMLR*, 2024. 3
- [40] Tsung-Yi Lin, Michael Maire, Serge Belongie, James Hays, Pietro Perona, Deva Ramanan, Piotr Dollár, and C Lawrence Zitnick. Microsoft coco: Common objects in context. In *ECCV*, 2014. 2, 3, 6
- [41] Bingchen Liu, Ehsan Akhgari, Alexander Visheratin, Aleks Kamko, Linmiao Xu, Shivam Shrirao, Joao Souza, Suhail Doshi, and Daiqing Li. Playground v3: Improving text-to-image alignment with deep-fusion large language models. *arXiv preprint arXiv:2409.10695*, 2024. 2, 3
- [42] Shilong Liu, Zhaoyang Zeng, Tianhe Ren, Feng Li, Hao Zhang, Jie Yang, Qing Jiang, Chunyuan Li, Jianwei Yang, Hang Su, et al. Grounding dino: Marrying dino with grounded pre-training for open-set object detection. *arXiv preprint arXiv:2303.05499*, 2023. 5, 1
- [43] Meta. Llama-3.1-8b-instruct. <https://huggingface.co/meta-llama/Llama-3.1-8B-Instruct>, 2024. 5, 6, 8, 1
- [44] Ben Mildenhall, Pratul P Srinivasan, Matthew Tancik, Jonathan T Barron, Ravi Ramamoorthi, and Ren Ng. Nerf: Representing scenes as neural radiance fields for view synthesis. *Communications of the ACM*, 2021. 3
- [45] OpenBMB. Minicpm-v-2.6. https://huggingface.co/openbmb/MiniCPM-V-2_6, 2024. 5, 8, 1, 2
- [46] William Peebles and Saining Xie. Scalable diffusion models with transformers. In *CVPR*, 2023. 2
- [47] Quynh Phung, Songwei Ge, and Jia-Bin Huang. Grounded text-to-image synthesis with attention refocusing. In *CVPR*, 2024. 3
- [48] Dustin Podell, Zion English, Kyle Lacey, Andreas Blattmann, Tim Dockhorn, Jonas Müller, Joe Penna, and Robin Rombach. Sdxl: Improving latent diffusion models for high-resolution image synthesis. In *ICLR*, 2024. 2, 8
- [49] Leigang Qu, Shengqiong Wu, Hao Fei, Liqiang Nie, and Tat-Seng Chua. Layoutllm-t2i: Eliciting layout guidance from llm for text-to-image generation. In *ACM MM*, 2023. 3
- [50] Alec Radford, Jong Wook Kim, Chris Hallacy, Aditya Ramesh, Gabriel Goh, Sandhini Agarwal, Girish Sastry, Amanda Askell, Pamela Mishkin, Jack Clark, et al. Learning transferable visual models from natural language supervision. In *ICML*, 2021. 3, 5
- [51] Colin Raffel, Noam Shazeer, Adam Roberts, Katherine Lee, Sharan Narang, Michael Matena, Yanqi Zhou, Wei Li, and Peter J Liu. Exploring the limits of transfer learning with a unified text-to-text transformer. *JMLR*, 2020. 3
- [52] Tianhe Ren, Qing Jiang, Shilong Liu, Zhaoyang Zeng, Wenlong Liu, Han Gao, Hongjie Huang, Zhengyu Ma, Xiaohe Jiang, Yihao Chen, et al. Grounding dino 1.5: Advance the "edge" of open-set object detection. *arXiv preprint arXiv:2405.10300*, 2024. 5, 1
- [53] Robin Rombach, Andreas Blattmann, Dominik Lorenz, Patrick Esser, and Björn Ommer. High-resolution image synthesis with latent diffusion models. In *CVPR*, 2022. 2
- [54] Chitwan Saharia, William Chan, Saurabh Saxena, Lala Li, Jay Whang, Emily L Denton, Kamyar Ghasemipour, Raphael Gontijo Lopes, Burcu Karagol Ayan, Tim Salimans, et al. Photorealistic text-to-image diffusion models with deep language understanding. In *NeurIPS*, 2022. 2
- [55] Tim Salimans, Ian Goodfellow, Wojciech Zaremba, Vicki Cheung, Alec Radford, and Xi Chen. Improved techniques for training gans. In *NeurIPS*, 2016. 5
- [56] Christoph Schuhmann, Romain Beaumont, Richard Vencu, Cade Gordon, Ross Wightman, Mehdi Cherti, Theo Coombes, Aarush Katta, Clayton Mullis, Mitchell Wortsman, et al. Laion-5b: An open large-scale dataset for training next generation image-text models. In *NeurIPS*, 2022. 3
- [57] Takahiro Shirakawa and Seiichi Uchida. Noisecollage: A layout-aware text-to-image diffusion model based on noise cropping and merging. In *CVPR*, 2024. 3
- [58] Jiaming Song, Chenlin Meng, and Stefano Ermon. Denoising diffusion implicit models. In *ICLR*, 2021. 2
- [59] stability.ai. Stable diffusion 3.5. <https://stability.ai/news/introducing-stable-diffusion-3-5>, 2024. 2, 3
- [60] Gemma Team, Thomas Mesnard, Cassidy Hardin, Robert Dadashi, Surya Bhupatiraju, Shreya Pathak, Laurent Sifre, Morgane Rivière, Mihir Sanjay Kale, Juliette Love, et al. Gemma: Open models based on gemini research and technology. *arXiv preprint arXiv:2403.08295*, 2024. 3, 5
- [61] Omost Team. Omost github page. <https://github.com/llyasviel/Omost>, 2024. 3, 5
- [62] Xudong Wang, Trevor Darrell, Sai Saketh Rambhatla, Rohit Girdhar, and Ishan Misra. Instancediffusion: Instance-level control for image generation. In *CVPR*, 2024. 2, 3, 4, 7, 8
- [63] Haohan Weng, Danqing Huang, Yu Qiao, Zheng Hu, Chinyew Lin, Tong Zhang, and CL Chen. Design: A pipeline for controllable design template generation. In *CVPR*, 2024. 3
- [64] Tsung-Han Wu, Long Lian, Joseph E Gonzalez, Boyi Li, and Trevor Darrell. Self-correcting llm-controlled diffusion models. In *CVPR*, 2024. 3, 5
- [65] Yinwei Wu, Xianpan Zhou, Bing Ma, Xuefeng Su, Kai Ma, and Xinchao Wang. Ifadapter: Instance feature control for grounded text-to-image generation. *arXiv preprint arXiv:2409.08240*, 2024. 3
- [66] Jiazheng Xu, Xiao Liu, Yuchen Wu, Yuxuan Tong, Qinkai Li, Ming Ding, Jie Tang, and Yuxiao Dong. Imagereward: Learning and evaluating human preferences for text-to-image generation. In *NeurIPS*, 2023. 5, 7
- [67] Han Xue, Zhiwu Huang, Qianru Sun, Li Song, and Wenjun Zhang. Freestyle layout-to-image synthesis. In *CVPR*, 2023. 3
- [68] Binbin Yang, Yi Luo, Ziliang Chen, Guangrun Wang, Xiaodan Liang, and Liang Lin. Law-diffusion: Complex scene generation by diffusion with layouts. In *ICCV*, 2023. 3, 5, 6
- [69] Ling Yang, Zhaochen Yu, Chenlin Meng, Minkai Xu, Stefano Ermon, and CUI Bin. Mastering text-to-image diffusion: Recaptioning, planning, and generating with multimodal llms. In *ICML*, 2024. 3, 5

- [70] Hu Ye, Jun Zhang, Sibao Liu, Xiao Han, and Wei Yang. Ip-adapter: Text compatible image prompt adapter for text-to-image diffusion models. *arXiv preprint arXiv:2308.06721*, 2023. [4](#)
- [71] Guangcong Zheng, Xianpan Zhou, Xuewei Li, Zhongang Qi, Ying Shan, and Xi Li. Layoutdiffusion: Controllable diffusion model for layout-to-image generation. In *CVPR*, 2023. [3](#), [5](#), [6](#)
- [72] Dewei Zhou, You Li, Fan Ma, Xiaoting Zhang, and Yi Yang. Migc: Multi-instance generation controller for text-to-image synthesis. In *CVPR*, 2024. [2](#), [3](#), [4](#), [7](#), [8](#)

CreatiLayout: Siamese Multimodal Diffusion Transformer for Creative Layout-to-Image Generation

Supplementary Material

A. More details on Datasets and Benchmarks

A.1. LayoutSAM Dataset and Benchmark

Layout annotation pipeline. We design a mechanism to automatically annotate the layout for any given image, as shown in Fig. 9.

I) Image Filtering: We employ the LAION-Aesthetics predictor [33] to assign aesthetic scores to images and filter out those with low scores. For SAM [30], we analyze the aesthetic scores shown in Fig. 10 and curate a high visual quality subset consisting of images in the top 50% of aesthetic scores.

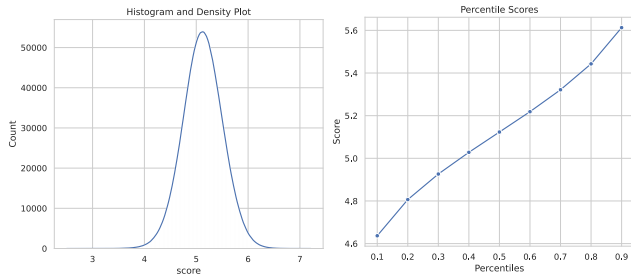


Figure 10. Distribution of aesthetic scores of SAM.

II) Global Caption Annotation: We generate the detailed

descriptions for the query image using the Qwen-VL-Chat-Dense-Captioner [16], which is a vision-language model fine-tuned on generative and human-annotated data using LoRA. This model supports accurate and detailed image descriptions. The average length of the captions is 95.41 tokens, measured by the CLIP tokenizer.

III) Entity Extraction: Existing state-of-the-art open-set grounding models [42, 52] perform better at detecting entities using a list of short phrases than directly using dense captions. Thus, we utilize the large language model Llama3.1-8b-it [43] to extract the main entities from dense captions via in-context learning. The brief descriptions include simple attribute descriptions with an average length of 2.08 tokens.

IV) Entity Spatial Annotation: We use Grounding DINO [42] to annotate bounding boxes of entities. To clean noisy data, we design the following filtering rules. We first filter out bounding boxes that occupy less than 2% of the total image area, then only retain images with 3 to 10 bounding boxes. The average number of entities per image is 3.96.

V) Region Caption Recaptioning: We use the vision language model MiniCPM-V-2.6 [45] to generate fine-grained descriptions with complex attributes for each entity based on its visual content and brief description. The generated detailed descriptions generally cover attributes such as color, shape, texture, and some text details, with an average length

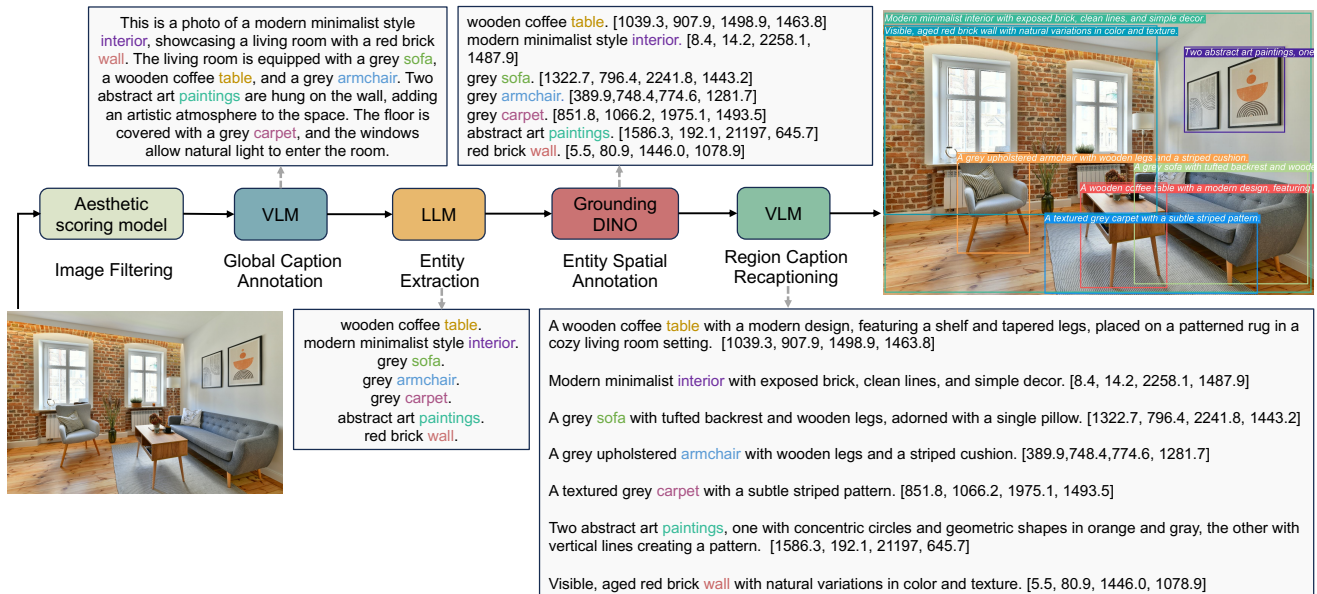


Figure 9. An overview of the proposed annotation pipeline, which can automatically annotate the layout information for any given image.

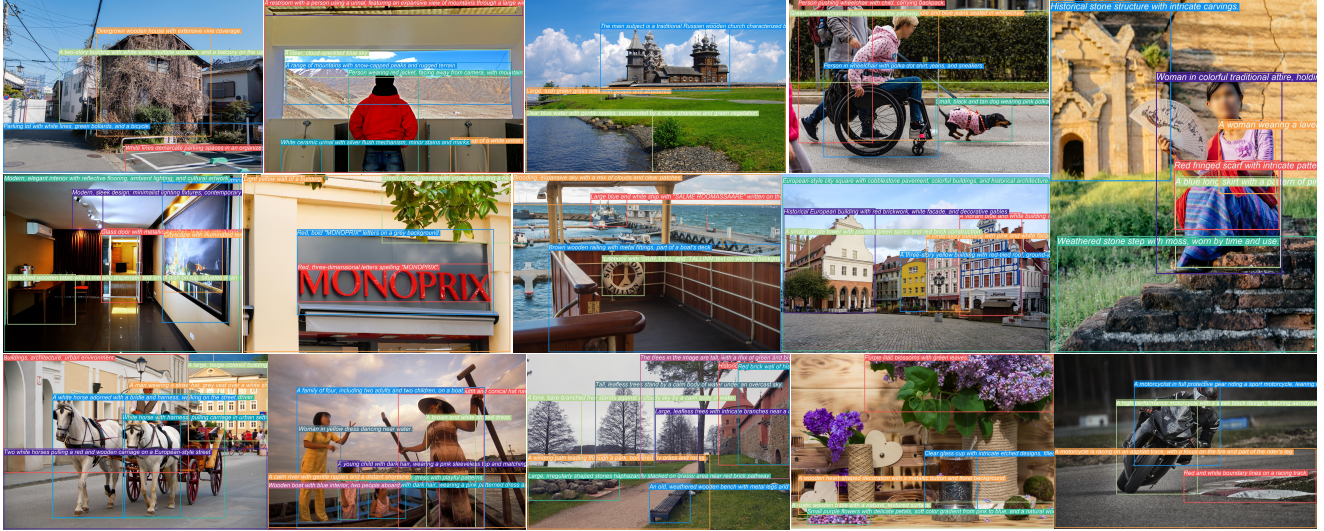


Figure 11. Examples from the LayoutSAM dataset.

of 15.07 tokens.

Finally, we contribute the large-scale layout dataset LayoutSAM, which includes 2.7 million image-text pairs and 10.7 million entities. Each entity is annotated with a bounding box and a detailed description. Fig. 11 shows some examples from LayoutSAM.

LayoutSAM-Eval Benchmark. The LayoutSAM-Eval benchmark, constructed from LayoutSAM, serves as a comprehensive tool for evaluating layout-to-image generation quality. It consists of 5,000 layout data points. We evaluate layout-to-image generation quality using LayoutSAM-Eval from two aspects: Spatial and Attribute, both of which are evaluated via the vision language model MiniCPM-V-2.6 [45] in a visual question-answering manner.

- *Spatial Accuracy.* To measure spatial adherence, for each bounding box, we ask the VLM whether the given entity exists within the bounding box, with the answer being either “Yes” or “No.” Finally, we divide the number of entities with a “Yes” answer by the total number of entities to obtain the spatial score.
- *Attribute Accuracy.* To measure attribute adherence, we ask the VLM whether the entity within the bounding box matches the attributes in the detailed description. For attributes like color, shape, and texture, each attribute is evaluated independently through visual question answering, and the score is obtained in the same manner as the spatial score.

A.2. Layout Planning Dataset and Benchmark

Layout Planning Dataset. To train LayoutDesigner, we construct a layout planning dataset derived from LayoutSAM. It consists of a total of 180,000 data points, covering

the following three tasks, each with 60,000 data points:

- *Caption-to-layout generation.* We randomly select data from LayoutSAM to construct pairs of global captions and ground truth layouts of entities. Each entity includes a bounding box and a description. This portion of the data is used to train the generation of layouts based on global captions.
- *Center point-to-layout generation.* For each entity, we calculate the center point from its bounding box to construct pairs of center points and ground truth layouts of entities. This portion of the data is used to train the generation of layouts based on the center points of entities.
- *Suboptimal layout-to-layout optimization.* For each entity, we create suboptimal layouts by performing operations such as deletion, duplication, movement, and resizing with a certain probability. This portion of the data consists of pairs of suboptimal layouts and GT layouts and is used to train the optimization of layouts from suboptimal to better.

LayoutDesigner is a unified layout planning model that supports all three tasks simultaneously through joint training of a large language model on these three types of data.

Layout Planning Benchmark. We construct 1,000 data points for each layout planning task using the same method from LayoutSAM-Eval and conduct experiments to evaluate layout planning capabilities under a 3-shot in-context learning setting. First, we evaluate the formatting accuracy of the generated layouts, including the coordinates of the top-left corner being smaller than those of the bottom-right corner and the bounding box not exceeding the image boundaries. To assess the harmony and aesthetics of the layouts, we did not use metrics like AP to measure the adherence of the generated bounding boxes to the ground truth. This is because

layout generation is an open-ended problem, and there can be multiple optimal solutions for the input. Even if a solution does not resemble the GT, it can still be an excellent layout. Therefore, we generate images based on the designed layouts and reflect the quality of the layouts through the quality of the images. Additionally, we evaluate the layout planning capabilities through qualitative results.

B. More analysis on modal competition

In Fig. 3, we analyze the issue of modality competition in M^3 -Attention: the similarity between the layout and the image is much lower than that between the global caption and the image. Our proposed SiamLayout alleviates this issue by decoupling it into two siamese MM-Attention branches: image-text and image-layout. We investigate the image-text and image-layout similarity scores in the attention map to further illustrate the modality competition, as shown in Fig. 12. The image-layout similarity score is determined by applying softmax to the attention map of the M^3 -Attention or image-layout MM-Attention, identifying the cross-region of the image and layout, and then taking the average of the top 1% scores in this cross-region. The image-text similarity score is calculated in the same way. Experimental results show that, as the training steps increase, the image-layout similarity score in M^3 -Attention remains consistently much lower than the image-text similarity score, resulting in the layout having a weaker influence on the image compared to the global caption. In contrast, due to the independent guiding role of the layout in the image-layout branch of SiamLayout, the image-layout similarity gradually increases to a value close to the image-text similarity as the network training progresses, thereby allowing the layout to play a more significant guiding role in image generation.

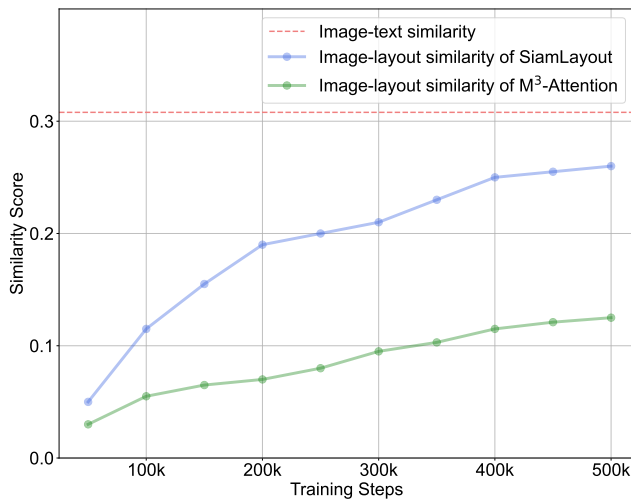


Figure 12. The trend of image-layout similarity in the attention maps of different network variants.

C. More qualitative results

We present more qualitative results in Fig. 13. Experimental results show that our proposed method empowers MM-DiT for layout-to-image generation, achieving visually appealing and precisely controllable generation, as demonstrated by the high adherence to complex attributes such as color, texture, and shape.



Figure 13. More qualitative results on layout-to-image generation.